Hyperons in the nuclear pasta phase

Débora P. Menezes
Depto de Física, CFM, Universidade Federal de Santa Catarina Florianópolis, SC, CP. 476, CEP 88.040-900, Brazil

Constança Providência*
CFisUC, Department of Physics, University of Coimbra, P3004-516 Coimbra, Portugal
(Received 5 July 2017; revised manuscript received 6 September 2017; published 9 October 2017)

We have investigated under which conditions hyperons (particularly Λs and Σ^-s) can be found in the nuclear pasta phase. As the density and temperature are larger and the electron fraction is smaller, the probability is greater that these particles appear, but always in very small amounts. Λ hyperons only occur in gas and in smaller amounts than would occur if matter were homogeneous, never with abundancies above 10^{-5}. The amount of Σ^- in the gas is at least two orders of magnitude smaller and can be disregarded in practical calculations.

DOI: 10.1103/PhysRevC.96.045803

I. INTRODUCTION

Not long ago, two massive stars were confirmed [1,2], giving rise to the hyperon puzzle: While nuclear physics favors soft equations of state (EOS) at low densities, massive stars can only be described by stiff EOS at high densities. Meanwhile, some constraints were imposed on neutron stars' radii and it is now believed that the radii of canonical 1.4 solar mass ($M_\odot$) pulsars are lower than what most of the models foresee [3].

On the other hand, the observation of supernova explosions is not trivial, a fact that contributed to the increasing importance of simulations of core-collapse supernova and its remnants. An appropriate EOS for these simulations would range from very low to high densities and from zero temperature to temperatures higher than 100 MeV, not a very easy task to accomplish. Hence, there is a very small number of these EOS on the market, most of them publicly available in the CompOSE (CompStar Online Supernovae Equations of State) database [4].

Many attempts have been made to circumvent these two problems and next we only mention some of the examples of the propositions found in the literature. These problems can be tackled by choosing appropriate meson-hyperon couplings [5] and introducing strange mesons as mediators of the baryons in relativistic models [6–9] in already existing models or by using combinations of different parts of models available in the literature [10]. In all cases, the existence of a degree of freedom that carries strangeness is important; see Ref. [11] for a recent review.

In this context, the low-density part of the EOS plays a role that cannot be disregarded. The nuclear pasta phase results from the competition between the strong and the Coulomb interactions at densities compatible with the ones in the inner crust of neutron stars. Such competition generates a frustrated system [12,13] and the name *pasta* refers to specific shapes acquired by matter, namely, droplets, bubbles, rods, tubes, and slabs. The inclusion of the pasta phase in the EOS practically does not influence the stellar maximum masses but certainly affects the radii [14,15]. So far, the pasta phase has only been treated with nucleonic degrees of freedom.

From the considerations made above, it is obvious that the constituents present in the equations of state (EOS) that describe neutron stars and supernova cores are the essential ingredients in the determination of thermodynamic quantities and macroscopic properties. Hence, the existence of the strangeness degree of freedom in the nuclear pasta phase has to be investigated and this is the aim of the present work. At zero temperature, hyperons do not occur at densities below two times the saturation density. However, at finite temperature, the appearance of hyperons is mainly governed by their mass and as the temperature increases, so does the probability that they will appear at smaller densities. We restrict our work to finite-temperature systems when the hyperons may occur at densities typical of nonhomogeneous matter. We first consider the possibility that Λ particles are present in the nuclear pasta phase, check the conditions for their existence, and later discuss situations that could give rise to the onset of Σ^- as well. These are the strangeness-carrying baryons that usually appear first in stellar matter due to the values of their masses. Typical density values of the hyperon onset in the homogeneous phase are given in the next section. The values encountered are used to justify the presence of hyperons in the pasta phase.

We next show only the most important formulas for the understanding of our calculations and then display the results alongside some comments and conclusions.

II. FORMALISM

We have chosen to describe hadronic matter within the framework of the relativistic non-linear Walecka model (NLWM) [16] with nonlinear terms [17]. In this model, the nucleons are coupled to the scalar σ, isoscalar-vector ω^μ, and isovector-vector $\vec{\rho}^\mu$ meson fields. We include a ω-ρ meson coupling term as in Refs. [14,18–21] because this term was shown to control the symmetry energy and its slope, resulting in equations of state that can satisfy most of the nuclear matter saturation properties and observational constraints. The

*cp@fis.uc.pt

Lagrangian density reads

$$\mathcal{L} = \sum_{j=1}^{4} \bar{\psi}_j [\gamma_\mu (i\partial^\mu - g_{\omega j}\,\omega^\mu - g_{\rho j}\,\vec{\tau}_j \,.\, \vec{\rho}^{\,\mu}) - m_j^*]\psi_j + \frac{1}{2}\partial_\mu\sigma\,\partial^\mu\sigma - \frac{1}{2}m_\sigma^2\sigma^2 - \frac{1}{3!}k\sigma^3 - \frac{1}{4!}\lambda\sigma^4 - \frac{1}{4}\Omega_{\mu\nu}\,\Omega^{\mu\nu} + \frac{1}{2}m_\omega^2\,\omega_\mu\omega^\mu - \frac{1}{4}\vec{R}_{\mu\nu}.\vec{R}^{\mu\nu} + \frac{1}{2}m_\rho^2\,\vec{\rho}_\mu \,.\, \vec{\rho}^{\,\mu} + \Lambda_{\rm v}\big(g_\rho^2\,\vec{\rho}_\mu \,.\, \vec{\rho}^{\,\mu}\big)\big(g_\omega^2\,\omega_\mu\omega^\mu\big)\,, \quad (1)$$

where $m_j^* = m_j - g_{\sigma j}\,\sigma$ is the baryon effective mass, $\Omega_{\mu\nu} = \partial_\mu\omega_\nu - \partial_\nu\omega_\mu$, $\vec{R}_{\mu\nu} = \partial_\mu\vec{\rho}_\nu - \partial_\nu\vec{\rho}_\mu - g_\rho(\vec{\rho}_\mu \times \vec{\rho}_\nu)$, g_{ij} are the coupling constants of mesons $i = \sigma,\omega,\rho$ with baryon j, and m_i is the mass of meson i. The couplings k ($k = 2\,M_N\,g_\sigma^3\,b$) and λ ($\lambda = 6\,g_\sigma^4\,c$) are the weights of the nonlinear scalar terms and $\vec{\tau}$ is the isospin operator. The sum over j extends over the lightest four baryons (n,p,Λ,Σ^-). In the present work, we have opted to use the NL3$\omega\rho$ parametrization [18], which is an extension of the NL3 parametrization [22] with the inclusion of the ω-ρ interaction. For the hyperon-ω interaction, we take SU(6) symmetry, and for the hyperon-σ interaction we consider that the Λ, Σ, and Ξ potentials in symmetric nuclear matter at saturation are, respectively, -28, $+30$, and -18 MeV. The parameters are $m_\sigma = 508.194$ MeV, $m_\omega = 782.501$ MeV, $m_\rho = 763$ MeV, $g_{\sigma n} = 10.217$ (n stands for protons and neutrons), $g_{\sigma\Lambda} = 6.323$, $g_{\sigma\Sigma} = 4.708$, $g_{\omega n} = 12.868$, $g_{\omega\Lambda} = g_{\omega\Sigma} = 8.578$, $g_{\rho j} = 11.276$, $k/M = 2 \times 10.431$, and $\lambda = -6 \times 28.885$, and the corresponding saturation properties are density at 0.148 fm^{-3}, binding energy of -16.2 MeV, compressibility equal to 271.6 MeV, symmetry energy of 31.7 MeV, and slope equal to 55.5 MeV. From the results in Ref. [23], one can see that this model predicts stellar masses above $2M_\odot$ and satisfies several presently accepted experimental and theoretical constraints.

The nuclear pasta phase is obtained for charge-neutral matter and leptons are usually incorporated because their presence is expected both in the interior of neutron stars and in the core-colapse supernova. The leptonic Lagrangian density is simply

$$\mathcal{L} = \bar{\psi}_l(i\gamma_\mu\partial^\mu - m_l)\psi_l, \quad (2)$$

where l represents only the e^- in the present work, whose mass is 0.511 MeV. The leptons enter the calculations only via the weak interaction.

The construction of the nuclear pasta phase obeys the well-known Gibbs conditions for phase coexistence and in the present work we opt for the coexistence phase (CP) method extensively discussed in previous works [12,14,24–26], which we do not repeat here. The particle chemical potentials are defined in terms of a baryon chemical potential (μ_B) and a charge chemical potential (μ_Q), which are the quantities enforced as identical in both phases, such as

$$\mu_j = \mu_B + q_j\mu_Q, \quad (3)$$

TABLE I. Hyperon onset densities obtained at zero temperature. Empty entries correpond to hyperon onsets above 1 fm^{-3}.

Y_e (MeV)	ρ_Λ (fm^{-3})	ρ_{Σ^+} (fm^{-3})	ρ_{Ξ^0} (fm^{-3})	ρ_{Ξ^-} (fm^{-3})
β-eq	0.31		0.64	0.35
0.1	0.30		0.61	0.34
0.30	0.33	0.77	0.60	
0.50	0.36	0.60	0.57	

where q_j is the electric charge of each particle. The electron fraction is fixed by the imposition of charge neutrality:

$$Y_e = \frac{\rho_e}{\rho} = Y_Q = \frac{\rho_Q}{\rho}, \quad \rho_Q = \rho_p - \rho_\Sigma. \quad (4)$$

We also define the fraction of Λ and Σ^- particles as

$$Y_{\Lambda_1} = \frac{\rho_{\Lambda_1}}{\rho}, \quad Y_{\Lambda_2} = \frac{\rho_{\Lambda_2}}{\rho}, \quad (5)$$

$$Y_{\Sigma_1} = \frac{\rho_{\Sigma_1}}{\rho}, \quad Y_{\Sigma_2} = \frac{\rho_{\Sigma_2}}{\rho}, \quad (6)$$

where the subscripts 1 and 2 refer to the dense phase and gas phase, respectively, and $\rho = \rho_p + \rho_n + \rho_\Lambda + \rho_\Sigma$. In most cases studied in this work, the Σ^- particles are not present. In this case, the density is given only by $\rho = \rho_p + \rho_n + \rho_\Lambda$ and $\rho_Q = \rho_p$.

An important aspect generally discussed is the surface tension coefficient (σ). We use the σ parametrization given in Ref. [26].

Before we discuss the presence of hyperons in the nuclear pasta phase, it is important to investigate their onset in homogeneous matter. We start by analyzing the two usually considered scenarios at zero temperature. The first one refers to stellar matter, where the equation of state is obtained with the assumption of charge neutrality and β equilibrium and the fraction of leptons includes electrons and muons, varies with density, and is an output of the calculation. In the second scenario, we have considered the electron fraction as a fixed quantity that enters as an input, as in the finite-temperature case examined throughout this work. In this case, no muons are incorporated in our calculations. As seen in Table I, no hyperons appear at subsaturation density at $T = 0$, as already expected. It is interesting to notice the competition between the contribution from the ρ meson that in asymmetric matter favors the hyperons with the smallest charges, and the σ meson that favors the hyperons with an attractive potential in symmetric nuclear matter at saturation. In symmetric matter, the ρ-meson contribution is zero, and the hyperons of each isospin multiplet with smaller mass are favored.

In Table II we display the onset of hyperons at different temperatures and electron fractions. We have considered the three hyperons with a larger fraction at low densities and we are interested in the occurrence of hyperons at densities below 0.1 fm^{-3}. From the table, we see that this is only possible for $T > 5$ MeV, taking as reference a hyperon fraction larger than 10^{-12}. While at very low T the sequence of hyperons may be different, at higher T the sequence is generally Λ, Σ,

TABLE II. Hyperon onset densities for hyperon fraction equal or above 10^{-12}. Only results for Λ, Σ^- and Ξ^- are shown. For $Y_e = 0.5$ the Ξ^0, Σ^+ and Σ^0 appear before, respectively, Ξ^- and Σ^- but the differences are small and the fractions are always very small.

T (MeV)	ρ_Λ (fm^{-3})	Y_Λ	ρ_{Σ^-} (fm^{-3})	Y_{Σ^-}	ρ_{Ξ^-} (fm^{-3})	Y_{Ξ^-}
$Y_e = 0.1$	Λ		Σ^-		Ξ^-	
0.001	0.31	10^{-12}		$<10^{-12}$	0.34	10^{-12}
1	0.28	10^{-12}	0.33	10^{-12}	0.32	10^{-12}
3	0.23	10^{-12}	0.28	10^{-12}	0.29	10^{-12}
5	0.13	10^{-12}	0.24	10^{-12}	0.26	10^{-12}
7	0	10^{-11}	0.18	10^{-12}	0.22	10^{-12}
9	0	$3.\times10^{-9}$	0	$5.\times10^{-12}$	0.17	10^{-12}
10	0	$2.\times10^{-8}$	0	$9.\times10^{-11}$	0.14	10^{-12}
12	0	$5.\times10^{-7}$	0	$6.\times10^{-9}$	0.03	10^{-12}
14	0	$4.\times10^{-7}$	0	$1.\times10^{-7}$	0	$2.\times10^{-11}$
$Y_e = 0.3$	Λ		Σ^-		Ξ^-	
0.001	0.33	10^{-12}		$<10^{-12}$		$<10^{-12}$
1	0.31	10^{-12}		$<10^{-12}$	0.56	10^{-12}
3	0.26	10^{-12}		$<10^{-12}$	0.40	10^{-12}
5	0.24	10^{-12}	0.34	10^{-12}	0.33	10^{-12}
7	0	10^{-11}	0.29	10^{-12}	0.29	10^{-12}
9	0	$3.\times10^{-9}$	0.21	10^{-12}	0.26	10^{-12}
10	0	$2.\times10^{-8}$	0	2×10^{-11}	0.23	10^{-12}
12	0	4×10^{-7}	0	10^{-9}	0.16	10^{-12}
14	0	3×10^{-6}	0	$3.\times10^{-8}$	0	$4.\times10^{-12}$
$Y_e = 0.5$	Λ		Σ^+		Ξ^0	
.001	0.37	10^{-12}	0.62	10^{-12}	0.60	10^{-12}
1	0.35	10^{-12}	0.59	10^{-12}	0.57	10^{-12}
3	0.30	10^{-12}	0.53	10^{-12}	0.50	10^{-12}
5	0.24	10^{-12}	0.47	10^{-12}	0.43	10^{-12}
7	0	$8.\times10^{-12}$	0.37	10^{-12}	0.38	10^{-12}
9	0	$2.\times10^{-9}$	0.34	10^{-12}	0.34	10^{-12}
10	0	10^{-8}	0.31	10^{-12}	0.32	10^{-12}
12	0	$2.\times10^{-7}$	0	$6.\times10^{-10}$	0.27	10^{-12}
14	0	$2.\times10^{-6}$	0	$3.\times10^{-9}$	0	10^{-12}

and Ξ. For a large electron fraction, close to $Y_e = 0.5$, the hyperon of the Σ triplet or Ξ doublet with the largest charge is the first to appear due to the smaller mass and the small contribution of the ρ meson. In fact, at $Y_e = 0.5$ the members of each isospin multiplet come very close together, being only distinguished by the mass. A small value of Y_e originates a large contribution from the ρ meson, and the hyperon with the most negative isospin projection is the favored one, i.e., Σ^- and Ξ^-. The differences among the hyperon optical potentials taken at $T = 0$ are washed out as the temperature rises, and, therefore, the Σ hyperon with a smaller mass than the Ξ hyperon ends up being favored. The Λ meson is always the one with the largest abundance, and we next concentrate our study in the occurrence of this hyperon. For reference, we also show some results for Σ but from Table II we conclude that when they occur at densities of the nuclear pasta phases they are 2 to 3 orders of magnitude less abundant than the Λs. The Ξ-hyperon fractions are negligible for the densities and temperatures where nuclear pasta phases occur.

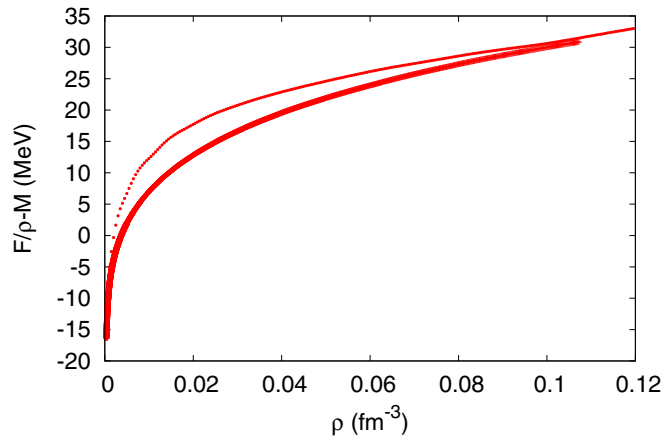

FIG. 1. Free energy vs baryon density for homogeneous matter (dotted line) and for the pasta phase (solid line) for $T = 10$ MeV and $Y_e = 0.3$.

III. RESULTS AND DISCUSSIONS

In the present section, we discuss under which conditions the fraction of hyperons, in particular, of Λs, is largest in the range of densities where nuclear pasta phases occur. The calculations are performed within the formalism presented in the last section. Although in the CP approach to the pasta phases, the surface energy and the Coulomb energy are added after the minimization of the free energy, we consider it is enough to get the correct idea of the amount of hyperons that occur in the nonhomogeneous subsaturation warm stellar matter. We perform the study within the NL3$\omega\rho$ parametrisation described in the last section.

We illustrate how the free energy per particle decreases when nonhomogeneous matter is considered instead of homogeneous matter in Fig. 1, taking $T = 10$ MeV and $Y_e = 0.3$. The range of densities where the nonhomogeneous matter occurs varies with temperature and electron fraction. In particular, it decreases as the temperature increases and eventually disappears above a certain critical temperature, which is around 14.45 MeV for this model [27]. Moreover, the electron fraction has a strong effect in the extension of the pasta phase: Since stellar matter is neutral, as the electron fraction increases so do theproton fraction and the nonhomogeneous matter extension.

In Fig. 2, the fraction of Λs is plotted as a function of (a) the electron fraction Y_e for $T = 10$ MeV and (b) the temperature for $Y_e = 0.3$. The dotted lines represent the fraction of Λs that would occur in homogeneous matter. In Fig. 2(a), the thick and the thin lines are the fractions of Λs with respect to the total density in the dense (cluster) and gas phases, as given in Eq. (5). Since there is no distillation effect for strangeness as there is for isospin [28], the larger (smaller) fraction in the dense (gas) phases simply reflects the fact that as the density gets larger, so does the probability that hyperons occur. Notice that under the conditions for pasta to occur these fractions are really very small. We may also conclude that the clusters contain no hyperons since the fraction is so small that it is not enough to predict a whole hyperon inside the clusters. This

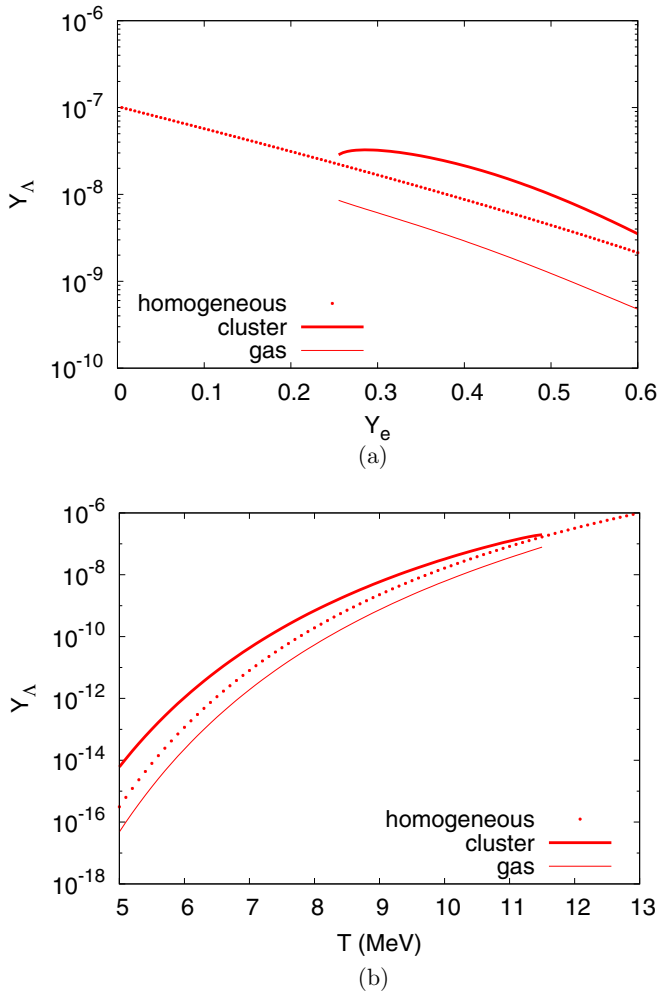

FIG. 2. Λ fractions obtained with with $\rho = 0.05\,\mathrm{fm}^{-3}$ as function of (a) the charge fraction at $T = 10$ MeV and (b) the temperature with $Y_e = 0.3$.

implies that in the nonhomogenous phase hyperons only occur in the gas and in smaller amounts than would occur if matter were homogeneous. This is illustrated in Fig. 3(a), where the black marks refer to the gas phase and the red ones refer to the dense phase.

Since the amount of strangeness seems to be so small, we have determined which conditions most favor the appearance of hyperons, taking the temperature between 4 and 14 MeV, the electron fraction between 0.05 and 0.6, and subsaturation densities; see Fig. 3. Hyperon fractions above 10^{-7} were possible only for $T > 10$ MeV. At these temperatures, nuclear pasta phases do not occur for too high or too low densities, or for too small electron fractions. However, as the electron fraction is smaller, the Λ fraction is larger at a given temperature, which is distinguishable by a color index, since these conditions favor the replacement of neutrons by Λs and decrease the free energy density.

There are, in fact, two competing factors related to the electron fraction: While more hyperons are favored with a smaller electron fraction to release the neutron pressure, the pasta extension is smaller for a smaller value of Y_e. As a result,

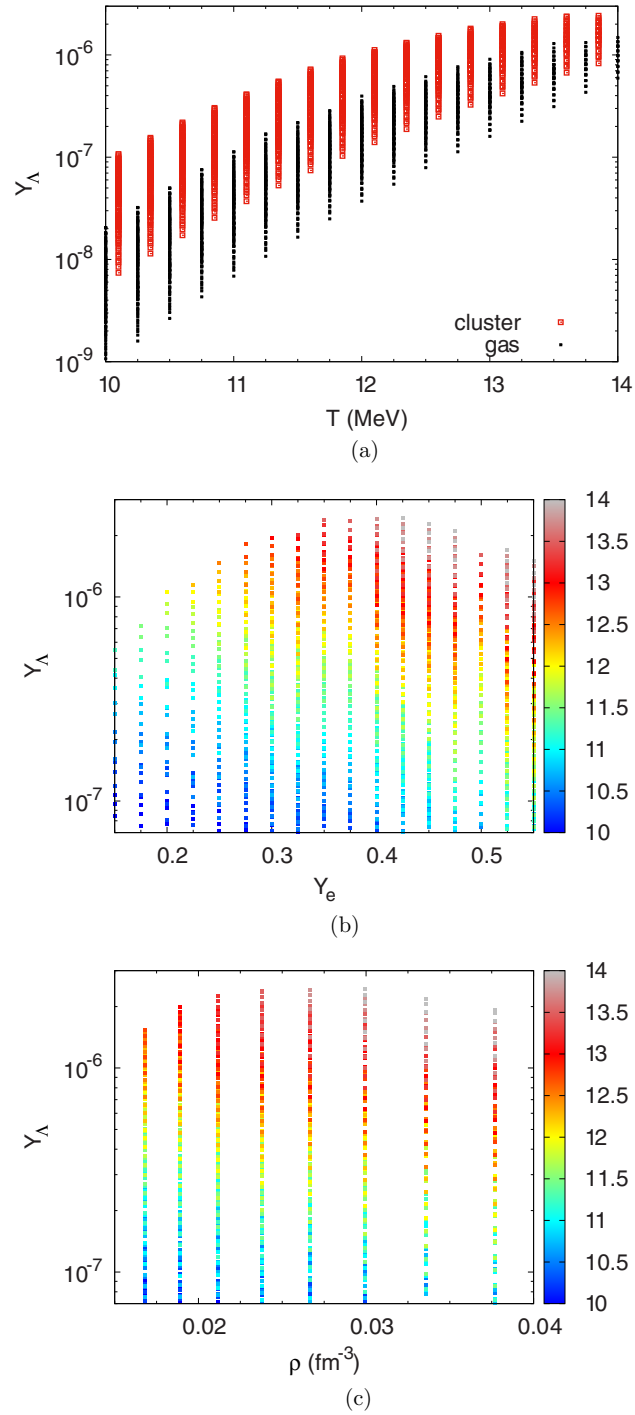

FIG. 3. Λ fraction as a function of (a) temperature in the clustered (red) and gas (black) phases; (b) electron fraction; (c) density under the conditions that predict fractions above 10^{-7}. In panel (a), to improve the visibility, the temperature of the clusters was shifted to the right by $\Delta T = 0.1$ MeV. In panels (b) and (c), only the Λ fractions in the clustered phase are shown, and temperature (in MeV) is indicated by a color index.

it is not possible to attain large temperatures with a small value of Y_e, and this explains the decrease of the Λ fraction with a decrease of Y_e if $Y_e < 0.35$, as seen in Fig. 3(b).

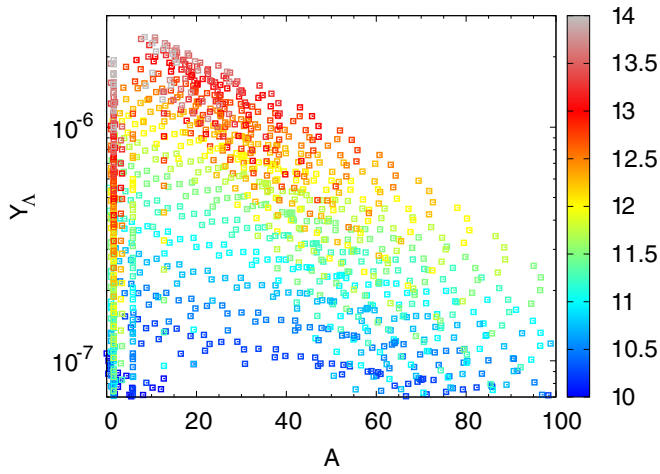

FIG. 4. Λ fraction as a function of the number of nucleons in the heavy clusters under the conditions that predict fractions above 10^{-7}. The temperature (in MeV) is indicated by a color index.

The internal structure of the nuclear pasta phase depends on the density, temperature, and amount of charged particles, and for $Y_s > 10^{-7}$ practically only droplets survive.

In the present calculation, only heavy clusters have been taken into account. The size of the clusters that occur under the conditions that favor hyperons can give important information. In Fig. 4, we illustrate the number of nucleons in the clusters for the Λ fractions above 10^{-7}. The largest fractions occur precisely for the smaller clusters. On the other hand, the present approach is not good enough to describe the nonhomogeneous matter at the boundary to the core and at the low density where the light clusters are most probable. The figure indicates that a study similar to the present one should be performed considering explicitly light clusters. Under these conditions, larger fractions of Λs as obtained in Ref. [29] are expected.

For the sake of completeness, we also allow for the presence of Σ^- particles, and their fraction is plotted in Fig. 5 as a function of (a) the electron fraction for $T = 10$ MeV alongside the fraction of Λs, (b) the temperature for $Y_e = 0.3$, and (c) the temperature for a range of densities between 0.015 and 0.035 fm^{-3} and electron fraction Y_e between 0.15 and 0.5. In Figs. 5(a) and 5(c), the Λ fraction is also displayed, so that the individual fraction of hyperons can be more easily compared. As seen from this figure and expected from the previous discussions, the amount of Σ^-s is almost negligible and can be disregarded in practical calculations. The Σ^- hyperons are the second to occur due to their charge and mass. Even though the repulsive potential of Σs in nuclear matter disfavors their appearance at finite temperature, for the small densities we consider the interaction plays a secondary role. The different behavior of the fraction of Λs and Σ^-s in nonhomogeneous and homogeneous matter can be attributed to the different isospin characters of these hyperons: (i) The Λs are not sensitive to isospin and their abundance is determined by the density, therefore a larger fraction is expected in denser matter and (ii) Σ^- has isospin projection -1 and is favored in asymmetric nuclear matter as the one occurring in the background gas of the nonhomogeneous matter. This explains

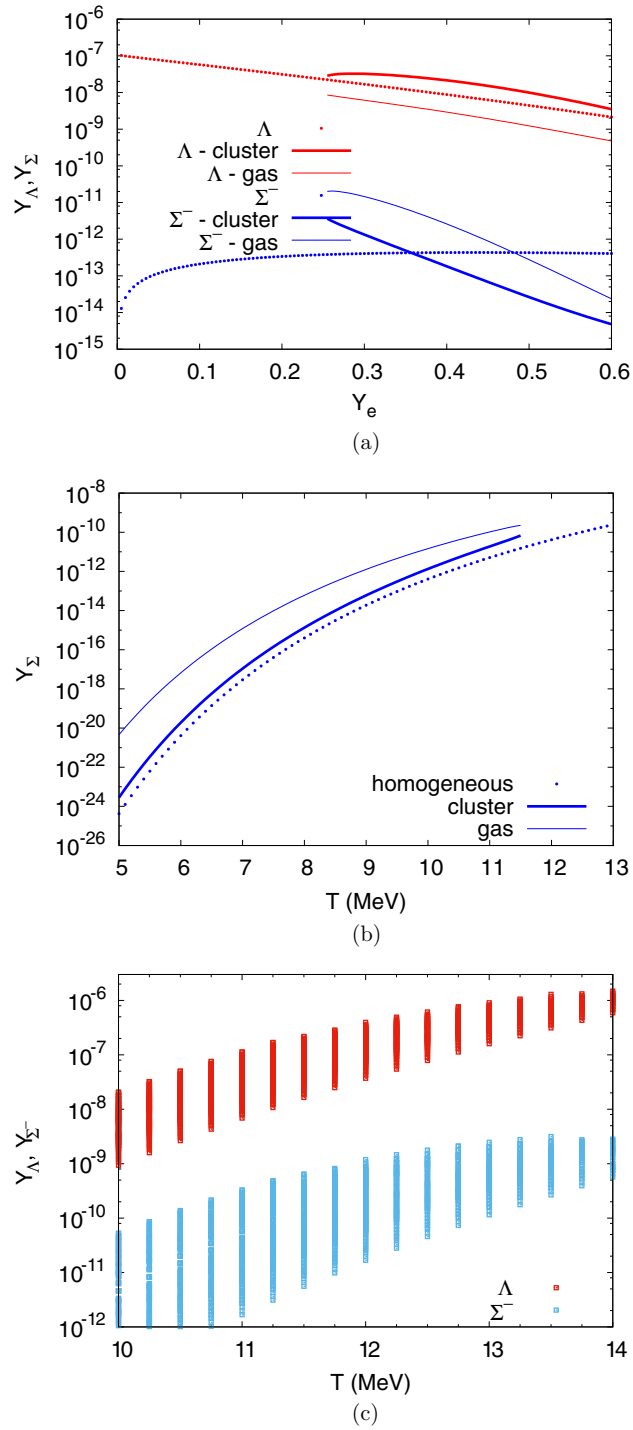

FIG. 5. Hyperon fractions obtained with $\rho = 0.05$ fm^{-3} as function of (a) the charge fraction at $T = 10$ MeV and (b) Y_Σ obtained as a function of the temperature with $Y_e = 0.3$. In panel (c) the fractions of Λs and Σ^-s are given as a function of temperature for a range of densities between 0.015 and 0.035 fm^{-3} and electron fraction Y_e between 0.15 and 0.5. Blue lines refer to Σs and red lines to Λs.

why the fraction of Σ^-s is larger in the gas phase. In Fig. 5(c), we compare the abundances of Λs and Σ^-s in the background gas, in the conditions that most favor the appearance of these

hyperons in the core-collapse supernova matter. It is seen that the Σ^-s fraction are essentially two orders of magnitude smaller than the Λ ones.

IV. CONCLUSIONS

We report a study on the presence of hyperons in the nonhomogeneous phase of core-collapse supernova matter. This was performed within the framework of a relativistic mean-field (RMF) EOS with properties compatible with the ones presently accepted. The nonhomogeneous phase was described within a coexisting phase approach which does not take into account in a self-consistent way the finite-size effects. However, the results obtained within this approach above $\rho \sim 0.01$ fm^{-3} give a prediction not far from a self-consistent Thomas Fermi calculation [30], and it is within this range of densities that the hyperons most contribute.

We have shown that the contribution of hyperons to the nonhomogeneous matter is generally negligible: The fraction of Λs obtained in all ranges of temperatures, densities, and electron fraction is always below 10^{-5}. The largest fractions occur for temperatures above 10 MeV, electron fractions between 0.3 and 0.5, and densities between 0.025 and 0.035 fm^{-3}. Other hyperons such as the Σ^- occur with two to six orders of magnitude smaller.

One interesting conclusion is that the heavy clusters carry no hyperons and the fraction of Λs in the gas phase is smaller than the expected fraction in homogeneous matter at the same density because these hyperons are not sensitive to the isospin distillation effect. On the other hand, Σ^-s are sensitive to isospin but in the best conditions their abundance is two to three orders of magnitude below the Λs abundance. This seems to indicate that the role of hyperons in matter with heavy clusters is negligible and can be taken into account by properly including hyperons in the background gas. A different problem concerns the appearance of hyperons together with light clusters which in the present study were not included: It was shown that the largest amounts of hyperons occur precisely with the smaller heavy clusters. Since our approach fails in the region of light clusters, a calculation taking these degrees of freedom into account should be performed.

ACKNOWLEDGMENTS

C.P. is thankful for the warm hospitality at Universidade Federal de Santa Catarina where this work was started. C.P. would also like to acknowledge discussions on the appearance of hyperons at low densities with F. Gulminelli and M. Oertel. This work was partially supported by Conselho Nacional de Desenvolvimento Científico e Tecnológico (CNPq), Brazil, under Grant No. 300602/2009-0; by Fundação para a Ciência e Tecnologia (FCT), Portugal, under Project No. UID/FIS/04564/2016; and by NewCompStar, a COST initiative.

[1] P. Demorest, T. Pennucci, S. Ransom, M. Roberts, and J. Hessels, Nature (London) **467**, 1081 (2010).
[2] J. Antoniadis *et al.*, Science **340**, 1233232 (2013).
[3] J. Lattimer and M. Prakash, Phys. Rept. **621**, 127 (2016).
[4] http://compose.obspm.fr
[5] M. Oertel, F. Gulminelli, C. Providência, and A. R. Raduta, Eur. Phys. J. A **52**, 50 (2016).
[6] I. Bednarek, P. Haensel, J. L. Zdunik, M. Bejger, and R. Manka, Astron. Astrophys. **543**, A157 (2012).
[7] S. Weissenborn, D. Chatterjee, and J. Schaffner-Bielich, Phys. Rev. C **85**, 065802 (2012).
[8] L. L. Lopes and D. P. Menezes, Phys. Rev. C **89**, 025805 (2014).
[9] L. L. Lopes and D. P. Menezes, arXiv:1701.03211 [nucl-th] (unpublished).
[10] M. Marques, M. Oertel, M. Hempel, and J. Novak, arXiv:1706.02913 [nucl-th] (unpublished).
[11] D. Chatterjee and I. Vidaña, Eur. Phys. J. A **52**, 29 (2016).
[12] S. S. Avancini, D. P. Menezes, M. D. Alloy, J. R. Marinelli, M. M. W. Moraes, and C. Providência, Phys. Rev. C **78**, 015802 (2008).
[13] J. Xu, L.-W. Chen, B.-A. Li, and H.-R. Ma, Phys. Rev. C **79**, 035802 (2009).
[14] G. Grams, A. M. Santos, P. K. Panda, C. Providência, and D. P. Menezes, Phys. Rev. C **95**, 055807 (2017).
[15] H. Pais, D. P. Menezes, and C. Providência, Phys. Rev. C **93**, 065805 (2016).
[16] B. D. Serot and J. D. Walecka, in *Advances in Nuclear Physics*, edited by J. W. Negele and E. Vogt (Plenum, New York, 1986), Vol. 16.
[17] J. Boguta and A. R. Bodmer, Nucl. Phys. A **292**, 413 (1977).
[18] C. J. Horowitz and J. Piekarewicz, Phys. Rev. Lett. **86**, 5647 (2001); Phys. Rev. C **64**, 062802 (2001); **66**, 055803 (2002).
[19] B. G. Todd-Rutel and J. Piekarewicz, Phys. Rev. Lett. **95**, 122501 (2005); F. J. Fattoyev and J. Piekarewicz, Phys. Rev. C **82**, 025805 (2010).
[20] F. J. Fattoyev, C. J. Horowitz, J. Piekarewicz, and G. Shen, Phys. Rev. C **82**, 055803 (2010).
[21] R. Cavagnoli, D. P. Menezes, and C. Providência, Phys. Rev. C **84**, 065810 (2011).
[22] G. A. Lalazissis, J. König, and P. Ring, Phys. Rev. C **55**, 540 (1997).
[23] M. Fortin, C. Providência, A. R. Raduta, F. Gulminelli, J. L. Zdunik, P. Haensel, and M. Bejger, Phys. Rev. C **94**, 035804 (2016).
[24] S. S. Avancini, S. Chiacchiera, D. P. Menezes, and C. Providência, Phys. Rev. C **85**, 059904(E) (2012).
[25] S. S. Avancini, C. C. Barros, D. P. Menezes, and C. Providência, Phys. Rev. C **82**, 025808 (2010).
[26] S. S. Avancini, C. C. Barros, L. Brito, S. Chiacchiera, D. P. Menezes, and C. Providência, Phys. Rev. C **85**, 035806 (2012).
[27] N. Alam, H. Pais, C. Providência, and B. K. Agrawal, Phys. Rev. C **95**, 055808 (2017).
[28] F. Gulminelli, Ad. R. Raduta, M. Oertel, and J. Margueron, Phys. Rev. C **87**, 055809 (2013).
[29] M. Oertel, M. Hempel, T. Klähn, and S. Typel, Rev. Mod. Phys. **89**, 015007 (2017).
[30] S. S. Bao, J. N. Hu, Z. W. Zhang, and H. Shen, Phys. Rev. C **90**, 045802 (2014).